AIP | Applied Physics Letters

Multi-scale patterning of microparticles using a combination of surface acoustic waves and ultrasonic bulk waves

Jie Zhang, Long Meng, Feiyan Cai, Hairong Zheng, and Charles R. P. Courtney

Citation: Applied Physics Letters **104**, 224103 (2014); doi: 10.1063/1.4881261
View online: http://dx.doi.org/10.1063/1.4881261
View Table of Contents: http://scitation.aip.org/content/aip/journal/apl/104/22?ver=pdfcov
Published by the AIP Publishing

Multi-scale patterning of microparticles using a combination of surface acoustic waves and ultrasonic bulk waves

Jie Zhang,[1,a),b)] Long Meng,[2,a)] Feiyan Cai,[2] Hairong Zheng,[2,b)] and Charles R. P. Courtney[3]
[1]*Department of Mechanical Engineering, University of Bristol, Bristol BS8 1TR, United Kingdom*
[2]*Paul C. Lauterbur Research Center for Biomedical Imaging, Institute of Biomedical and Health Engineering, Shenzhen Institutes of Advanced Technology, Chinese Academy of Sciences, Guangdong 518055, People's Republic of China*
[3]*Department of Mechanical Engineering, University of Bath, Bath BA2 7AY, United Kingdom*

(Received 28 February 2014; accepted 21 May 2014; published online 3 June 2014)

Standing surface acoustic waves (SAWs) and standing bulk waves (BWs) are combined to pattern two populations of particles with differing sizes. Patterns with large differences in wavelength in each direction and simultaneous generation of different patterns for each population are demonstrated. Particles are trapped at nodal positions of orthogonal standing wave fields in patterns determined by device voltage amplitudes and frequencies. 10-μm beads are trapped at points at the intersection of the pressure nodes of the SAW and BW fields, and 1-μm beads are trapped in lines at the pressure nodes of the SAW field, producing a multi-scale pattern. © *2014 Author(s). All article content, except where otherwise noted, is licensed under a Creative Commons Attribution 3.0 Unported License.* [http://dx.doi.org/10.1063/1.4881261]

When a particle in a fluid is insonated by an ultrasound field, an acoustic radiation force is generated by the interaction between the incident and scattered ultrasound.[1] In an ultrasonic standing wave field, the acoustic radiation force can trap particles in a potential energy well. Depending on the material properties of the particle and fluid, this potential well coincides with either a pressure node or a pressure anti-node of the field. An ultrasonic standing wave can be generated from either one ultrasonic source with a reflector[1–8] or two opposing sources.[6,9–14] Generally, the ultrasonic source is either a piezo-ceramic transducer generating a bulk wave (BW)[2–5,7–10,13,14] or a surface acoustic wave (SAW) device such as an inter-digital transducer (IDT) etched on single-crystal lithium niobate ($LiNbO_3$).[6,11,12] The former has been used to generate standing planar waves with the frequency usually ranging from 100 kHz to 10 MHz,[3] and the latter in the usual frequency range from 20 MHz (Ref. 6) to 40 MHz.[11,12] Standing bulk waves at 25 MHz have been used to trap particles,[15] but operation at these frequencies is unusual due to the difficulties of streaming and alignment. Very-high-frequency focused transducers operating at up to 200 MHz BW have been used to trap single particles at the focal point of the beam,[16,17] but do not generate the long length-scale patterning that is exploited in standing wave devices.

In both BW and SAW devices, particles can be trapped at either pressure nodes or anti-nodes depending on the material properties of the particles and fluid within the device. In the resultant patterns, the separation between neighboring lines of particles (the nodal spacing) is of the order of a half wavelength, and these patterns form lines or regular polygons depending on the transducer layout.[14] This offers a non-contact way of particle trapping,[18] sorting,[2] patterning, and manipulation in fluids with a minimum of mechanical stress.[3–6,9–11] These techniques have been used for cell agglomeration,[19] selection[7] and bioassays,[8] and microbubble patterning[12] as well as composite fabrication.[13] In these applications, there is a demand for more control over complex patterning and manipulation of multiple types of particles in the same chamber to investigate their interaction and fabricate new materials. Some of these demands have been realized using lithographic technologies with limited manipulation capability, e.g., multi-scale patterns of proteins[20] and nanofibers[21] for biological cell adhesion and solar cell fabrication. Similar functions achieved by ultrasound will increase its patterning and manipulation capabilities and extend applications in biological and life science and material engineering.

In this Letter, we use a combination of BW and SAW devices to trap particles of two different sizes in a multi-scale pattern. Here, the multi-scale pattern refers to a multi-scale nodal spacing resulting in an irregular polygonal pattern, and a difference of acoustic radiation force which can be used to trap particles of two different sizes in different node locations. Due to their large operating frequency difference, the combination of BW and SAW devices can provide larger differences in nodal spacing and magnitude of acoustic radiation force than combinations of a single type of device. Although orthogonal BWs of differing frequency could be used to generate patterns with differing scales in each direction, the aspect ratio is limited by the frequency range at which trapping can be achieved. At low frequencies (below 2 MHz), micrometer-scale particles are difficult to trap limiting the range of frequencies available and hence the possible ratio of wavelengths in each direction. Here, it is demonstrated that by combining SAWs and BWs, an aspect ratio of more than 6:1 can be achieved even when trapping 1-μm beads using moderate pressure amplitudes. The technical problem is to combine wave modes from BW and SAW devices in a chamber. The solution will provide the possibility of using different wave

[a)]Jie Zhang and Long Meng contributed equally to this work.
[b)]Authors to whom correspondence should be addressed. Electronic addresses: j.zhang@bristol.ac.uk and hr.zheng@siat.ac.cn

modes to select, separate, pattern, and manipulate different particles, which will benefit the understanding of the interaction between different particles and the fabrication of multi-layer multi-functional structures. This will improve the range of pattern that ultrasound can produce, and hence move ultrasound to the point where it can start to rival lithography.

For a particle significantly smaller than the wavelength, λ, in a plane acoustic standing-wave field with a given pressure amplitude in an inviscid fluid, the primary acoustic radiation force scales with $1/\lambda$.[22–25] This indicates that SAW (typically operating at wavelengths longer than 300 μm (Refs. 2–5, 7–10, 13, and 14)) and BW (typically operating at wavelengths shorter than 200 μm (Refs. 6, 11, and 12) devices perform similar particle trapping and patterning functions, but produce different acoustic force amplitudes and nodal spacing scales. Combining SAW and BW devices which cover a wide range of frequencies is therefore a potential method for producing patterns with multi-scale features. In such combined devices, operating voltage amplitude and frequency should ensure that the acoustic radiation force contributed by one device can overcome acoustic streaming[26,27] and viscous drag forces in the fluid for all particles, but the other device can do it only for the larger particles in the population.

Fig. 1 shows the combined device used for generating multi-scale patterns of particles. The device is attached to a printed circuit board, an IDT is etched on a $LiNbO_3$ substrate, and a lead zirconate titanate (PZT) plate is placed orthogonally to one side of the $LiNbO_3$ substrate. A PDMS block is located on the $LiNbO_3$ substrate at the intersection of the two orthogonal waves. There is a cylindrical chamber inside the PDMS block which contains the fluid and particles. The center of this chamber is the origin of a Cartesian coordinate system. The ultrasonic waves from the PZT plate were coupled into the PDMS fluid system through a thin water layer. An IDT located opposite a PDMS outside wall is used to generate a standing SAW propagating along the x direction and a PZT plate with another PDMS outside wall is used to generate a standing BW propagating along the y direction.

It is known that the propagation of SAWs excited by IDTs on a piezoelectric substrate can be simulated by plane waves propagating with frequency-dependent attenuation.[6] Here, SAW attenuation is ignored due to short propagation distance in the device, and it is assumed that the standing

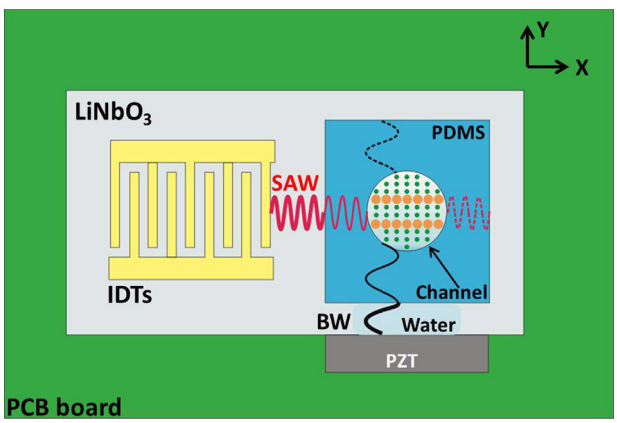

FIG. 1. Schematic diagram of the combined SAW and BW device.

SAW and standing BW are composed of an incident wave and a wave reflected from the PDMS outside walls.[6] When the reflection coefficients from the PDMS outside walls along x and y directions are $R_x = R_y = -1$, the resultant time averaged pressure amplitude in the fluid chamber is

$$\langle |P_x + P_y|^2 \rangle = 4[P_{x0}^2 \sin^2(k_x x - k_x a - k_b l) + P_{y0}^2 \sin^2(k_y y - k_y a - k_y m)], \quad (1)$$

where the subscripts x and y represent the waves propagation in x and y directions, respectively, and the subscript b means the longitudinal wave propagation in the PDMS block. P_{x0} and P_{y0} are the amplitudes of incident waves, the wavenumber $k = 2\pi/\lambda$, a is the radius of the fluid filled chamber, and l and m are the distances from the chamber edges to the PDMS outside walls at the x and y directions, respectively. From Eq. (1), in this orthogonal standing wave field, the pressure nodal separations are half the wavelength in the x and y directions. Equation (1) also indicates that P_{x0} and P_{y0} directly affect the particle pattern, and this is similar to the work done by Oberti.[28] Therefore, P_{x0} and P_{y0} need to be measured in order to allow particle patterns to be generated as designed using the combined device. P_{x0} and P_{y0} can be experimentally measured using the well-known particle trajectory approach.[23,24]

A prototype device has been fabricated. The IDT is made of 200 nm aluminum etched on 0.5 mm thick 128° Y-X-axis-rotated cut and X-propagating $LiNbO_3$ crystal substrate. This IDT has 40 straight finger pairs with space ratio of 1:1, a width of 20 μm, and an aperture size of 9 mm, and operates at $f_x = 39.2$ MHz with corresponding wavelength of $\lambda_x = 100$ μm.[12] A 2×15 mm PZT plate with a thickness of 0.975 mm was chosen for generating bulk waves with $f_y = 2.3$ MHz and $\lambda_y = 643$ μm in water. A cylindrical chamber was fabricated in a PDMS (Sylgard 184, Dow Corning, USA) block with a size of $6 \times 2.5 \times 2.5$ mm^3. Compared to a square or rectangular shape hole, a circular hole in PDMS requires less alignment to the wave incident direction when bonding with a substrate and is therefore used in the prototype device. The chamber has a height of 50 μm, a radius of $a = 0.6$ mm, and the distance from its edges to the PDMS outside wall at x_0 and y_0 are $l = 1.2$ mm and $m = 2.1$ mm. The primary acoustic radiation force on a compressible sphere in an inviscid fluid scales with $1/\lambda$,[22–25] so in this combined device, the standing SAW should provide 6.4 times the primary acoustic radiation force amplitude as the standing BW for a given particle and acoustic pressure. In this device, $R_x = R_y \approx -1$ and Eq. (1) can be used to model the acoustic pressure field.

Fig. 2 shows the estimated total pressure distribution from standing waves operating at frequencies of $f_x = 39.2$ MHz and $f_y = 2.3$ MHz under different pressure amplitude ratios, P_{x0}/P_{y0}. Fig. 2(a) shows a rectangular pattern with the separation distance of $\Delta x = \lambda_x/2 = 50$ μm and $\Delta y = \lambda_y/2 = 320$ μm. Larger pressure amplitude ratios cause different pressure gradients in each direction, and this can change a rectangular pattern to a line pattern as shown in Fig. 2(b). From Figs. 2(a) and 2(b), it can be seen that in order to generate a rectangular pattern, it is necessary to make sure $P_{x0}/P_{y0} \approx 1$. It is therefore necessary that P_{x0} and P_{y0} be first experimentally

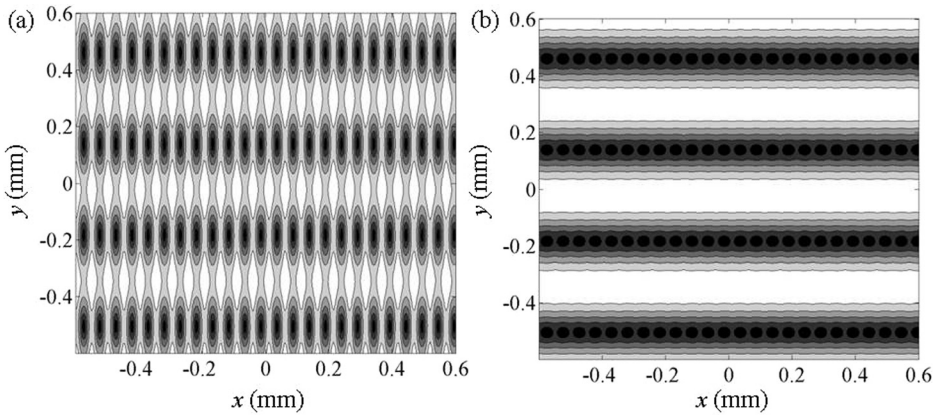

FIG. 2. Simulated total pressure amplitude from two orthogonal standing waves ($f_x = 39.2$ MHz and $f_y = 2.3$ MHz) from Eq. (1) and using, (a) $P_{x0}/P_{y0} = 1$ and (b) $P_{x0}/P_{y0} = 5$. The scale runs from black at 0 to white at maximum pressure amplitude.

measured and then used to set the ratio of operating voltages of the SAW and BW devices.

In the experimental measurements, the pressure amplitudes of the standing wave from the IDT or the PZT plate in the combined device were measured separately: with only one source operating in each experiment. Sinusoidal waves with the same peak-to-peak voltage of 10 V were used for each transducer, but with frequencies (i.e., 39.2 MHz and 2.3 MHz) appropriate to the transducer. In each measurement, a solution of particles was injected into the PDMS chamber using a syringe pump (KDS-270-CE, KD Scientific, Hollistion, USA). 10 μm diameter polystyrene spherical beads ($r = 5$ μm, $\rho_m = 1062$ kg/m^3, and $c_m = 2400$ m/s) were chosen for calculating the primary acoustic radiation force amplitude, due to $r \ll \lambda$. The trajectories of the 10-μm beads in water ($\mu = 0.001002$ Pa s) in the PDMS chamber were tracked and trajectories with transverse movement longer than $\lambda/4$ were then used to calculate the acoustic radiation force amplitude using the particle trajectory approach.[23,24] The measurements were repeated 40 times for each transducer, and Fig. 3 shows the distributions of the measured acoustic radiation force amplitude for the 10-μm beads in the standing SAW and standing BW fields. The variation of the measured ARF may be caused by pressure and temperature variation in the chamber and acoustic streaming disturbance. The forces due to the SAW demonstrate more variation than those due to the BW. Further investigation is required, but this variation may reflect greater spatial variations in the field for the short wavelength SAW waves. The averaged acoustic radiation force amplitude on a 10-μm bead from the standing SAW and the standing BW are 4.8 pN and 1.5 pN, respectively, which corresponds to $P_{x0} = 22$ kPa and $P_{y0} = 30$ kPa based on the analytical model of the acoustic radiation force for small particles[22–25] and the particle trajectory approach.[23,24] The voltage amplitude is assumed to be linearly proportional to pressure and so a SAW: BW voltage ratio of 1.4:1 was used. The IDT and the PZT plate were excited simultaneously at, with voltages of 10 V and 7 V, respectively, and the experimentally trapped 10-μm beads are shown in Fig. 4(a). As intended a rectangular pattern with $\Delta x \approx 50$ μm and $\Delta y \approx 320$ μm is produced. This shows a good agreement with the simulated pressure distribution shown in Fig. 2(a).

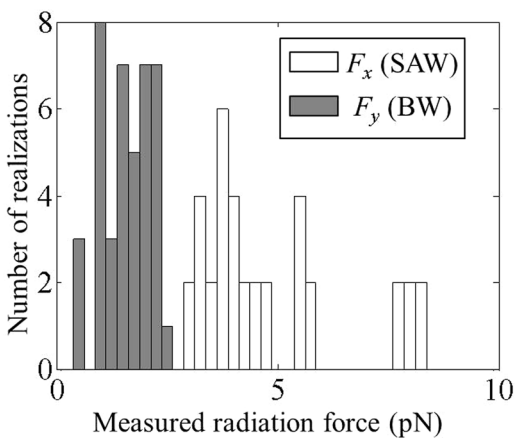

FIG. 3. Histograms of experimentally measured acoustic radiation force amplitude on 10-μm-diameter polystyrene spherical beads in the field generated by the SAW device and the field generated by the BW device.

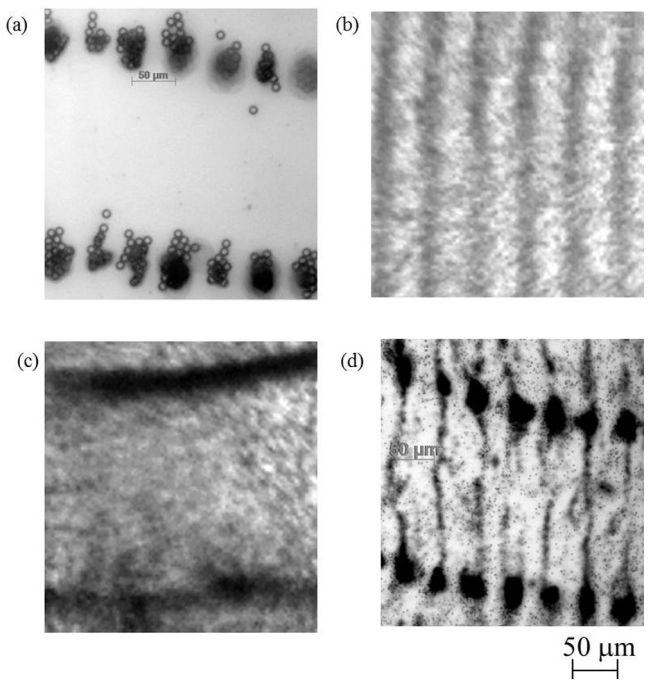

FIG. 4. Experimental patterns from the combined device for, (a) 10-μm-diameter polystyrene spherical beads patterned using the SAW and the BW devices at 10 V and 7 V, respectively, (b) 1 μm diameter polystyrene spherical beads only using the SAW device at 9 V, (c) 1-μm-diameter polystyrene spherical beads trapped using only the BW device at 20 V, and (d) mixed 1-μm and 10-μm-diameter polystyrene spherical beads patterned using the SAW device and the BW device simultaneously at 10 V and 7 V. The microscope magnification is 200.

1-μm-diameter polystyrene spherical beads, due to the lower acoustic radiation force, are much more difficult to trap and track. Instead the minimum voltages for trapping 1-μm beads using the SAW device and the BW device were measured experimentally by stepwise changing the voltage from 1 V to 25 V. It was found that the lowest peak-to-peak voltage amplitudes to trap the 1-μm beads were 9 V and 20 V for the IDT and the PZT plate devices, respectively. The line-like patterns generated by separately operating the IDT and PZT at the appropriate minimum voltages are shown in Figs. 4(b) and 4(c), respectively. These measured minimum voltages indicate that if the operating voltage is between 9 V and 20 V 1-μm beads will only be trapped by the standing SAW field. Fig. 4(d) shows the multi-scale pattern for the mixed 1-μm and 10-μm beads under the operating voltages of 10 V and 7 V for the IDT and the PZT plate. In this pattern, the 1-μm beads are trapped at the same nodal lines of the standing SAW as when only the IDT is active (indicating that the beads are trapped by the acoustic radiation force and not streaming), and the 10-μm beads are trapped at the grid points determined by the nodes of both standing waves.

In summary, it is demonstrated that standing SAWs and standing BWs can work together to generate a multi-scale patterns using a SAW device (IDT) combined with a BW device (PZT plate) operating at suitable frequencies and voltages. The different operation frequencies for the IDT and the PZT plate produce a rectangular (spatially multi-scale) pressure node distribution with a large aspect ratio and different particle trapping capability for each transducer in a given pressure field. The experimental results demonstrated that operation at 10 V and 7 V for the IDT, and the PZT plate leads to the generation of the multi-scale patterns for mixed 1-μm and 10-μm-diameter polystyrene spherical beads: where 1-μm beads are trapped in lines, and 10-μm beads are trapped on a grid of points. The experimental multi-scale pattern demonstrates the potential for particle patterning, selection, and separation with one device combining SAWs and BWs and suggests how patterning and manipulation strategies in microfluidic and acoustic tweezer devices may develop in future.

The work was supported by the EPSRC of United Kingdom (Grant No. EP/G012067/1), and National Science Foundation of China (Grant Nos. 11304341, 11302239, 11274008, 61020106008, and 11325420).

[1]H. Bruus, Lab Chip **12**, 1014 (2012).
[2]A. D. Johnson and L. D. Feke, Sep. Technol. **5**, 251 (1995).
[3]T. Laurell, F. Petersson, and A. Nilsson, Chem. Soc. Rev. **36**, 492 (2007).
[4]P. Glynne-Jones, R. J. Boltryk, N. R. Harris, A. W. Cranny, and M. Hill, Ultrasonics **50**, 68 (2010).
[5]P. Glynne-Jones, C. E. M. Demore, C. W. Ye, Y. Q. Qiu, S. Cochran, and M. Hill, IEEE Trans. Ultrason. Ferroelectr. Freq. Control **59**, 1258 (2012).
[6]J. J. Shi, D. Ahmed, X. Mao, S. S. Lin, A. Lawit, and J. T. Huang, Lab Chip **9**, 2890 (2009).
[7]P. Rogers, I. Gralinski, C. Galtry, and A. Neild, Microfluid. Nanofluid. **14**, 469 (2013).
[8]M. Evander, L. Johansson, T. Lilliehorn, J. Piskur, M. Lindvall, S. Johansson, M. Almqvist, T. Laurell, and J. Nilsson, Anal. Chem. **79**, 2984 (2007).
[9]A. Grinenko, C. K. Ong, C. R. P. Courtney, P. D. Wilcox, and B. W. Drinkwater, Appl. Phys. Lett. **101**, 233501 (2012).
[10]C. R. P. Courtney, C. K. Ong, B. W. Drinkwater, A. L. Bernassau, P. D. Wilcox, and D. R. S. Cumming, Proc. R. Soc. London, Ser. A **468**, 337 (2012).
[11]C. D. Wood, J. E. Cunningham, R. O'Rorke, C. Wälti, E. H. Linfield, A. G. Davies, and S. D. Evans, Appl. Phys. Lett. **94**, 054101 (2009).
[12]L. Meng, F. Cai, Q. Jin, L. Niu, C. Jiang, Z. Wang, J. Wu, and H. Zheng, Sens. Actuator, B **160**, 1599 (2011).
[13]M. S. Scholz, B. W. Drinkwater, and R. S. Trask, Ultrasonics **54**, 1015 (2014).
[14]A. L. Bernassau, C. R. P. Courtney, J. Beeley, B. W. Drinkwater, and D. R. S. Cumming, Appl. Phys. Lett. **102**, 164101 (2013).
[15]Y. Qiu, C. Demore, S. Sharma, S. Cochran, D. A. Hughes, and K. Weijer, in *Proceedings of the IEEE International Ultrasonics Symposium (IUS) 2011, Orlando, USA, 18–21 October* (2011), pp. 188–191.
[16]H. Hsu, F. Zheng, Y. Li, C. Lee, Q. Zhou, and K. K. Shung, Appl. Phys. Lett. **101**, 024105 (2012).
[17]J. Lee, C. Lee, H. H. Kim, A. Jakob, R. Lemor, S. Teh, A. Lee, and K. K. Shung, Biotechnol. Bioeng. **108**, 1643 (2011).
[18]M. Evander and J. Nilsson, Lab Chip **12**, 4667 (2012).
[19]T. W. Coakley, J. J. Hawkes, A. M. Sobanski, M. C. Cousins, and J. Spengler, Ultrasonics **38**, 638 (2000).
[20]Y. Li, G. He, S. Wang, S. Yu, F. Pan, H. Wu, and Z. Jiang, J. Mater. Chem. A **1**, 10058 (2013).
[21]S. Hwang, C. Kim, H. Song, S. Son, and J. Jang, ACS Appl. Mater. Interfaces **4**, 5287 (2012).
[22]L. P. Gor'kov, Sov. Phys. Dokl. **6**, 773 (1962).
[23]M. Gröschl, Acustica **84**, 432 (1998).
[24]R. Barnkob, P. Augustsson, T. Laurell, and H. Bruus, Lap Chip **10**, 563 (2010).
[25]K. Yosioka and Y. Kawasima, Acustica **5**, 167 (1955).
[26]J. F. Spengler, W. T. Coakley, and K. T. Christensen, AICHE J. **49**, 2773 (2003).
[27]S. K. R. S. Sankaranarayanan, S. Cular, V. R. Bhethanabotla, and B. Joseph, Phys. Rev. E **77**, 066308 (2008).
[28]S. Oberti, A. Neild, and J. Dual, J. Acoust. Soc. Am. **121**, 778 (2007).